한국소음진동공학회논문집 제17권 제9호, pp. 835~846, 2007.

Parametric Studies of Flexural Free Vibrations of Circular Strip Foundations with Various End Constraints Resting on Pasternak Soil

경계조건 변화에 따른 Pasternak지반으로 지지된 원호형 띠기초의 휨 자유진동에 관한 변수연구

Byoung Koo Lee†, Li Guangfan*, Hee Jong Kang** and Hee Min Yoon**
이 병 구·李 光 范·강 희 종·윤 희 민

(Received June 11, 2007 ; Accepted August 7, 2007)

Key Words : Flexural Free Vibration(휨 자유진동), Natural Frequency(고유진동수), Circular Strip Foundation (원호형 띠기초), Variable Breadth(변화폭), Pasternak Soil(Pasternak 지반)

ABSTRACT

This paper deals with the flexural free vibrations of circular strip foundation with the variable breadth on Pasternak soil. The breadth of strip varies with the linear functional fashion, which is symmetric about the mid-arc. Differential equations governing flexural free vibrations of such strip foundation are derived, in which the elastic soil with the shear layer, i.e. Pasternak soil, is considered. Effects of the rotatory and shear deformation are included in the governing equations. Differential equations are numerically solved to calculate the natural frequencies and mode shapes. In the numerical examples, the hinged-hinged, hinged-clamped and clamped-clamped end constraints are considered. Four lowest frequency parameters accompanied with their corresponding mode shapes are reported and parametric studies between frequency parameters and various system parameters are investigated.

요 약

이 논문은 Pasternak 지반으로 지지된 변화폭 원호형 띠기초의 휨 자유진동에 관한 연구이다. 단면폭은 띠기초의 중앙점을 중심으로 대칭 일차 함수를 갖는 변화폭으로 선정하였다. 이 연구에서 지반은 전단층을 갖는 탄성지반인 Pasternak 지반으로 모형화 하였고 회전관성과 전단변형을 고려한 곡선 띠기초의 자유진동을 지배하는 상미분방정식을 유도하였다. 이 상미분방정식을 수치해석하여 고유진동수 및 진동형을 산출하였다. 수치해석 예에서는 회전-회전, 회전-고정 및 고정-고정의 3개의 지점조건을 고려하였다. 띠기초의 무차원 변수들이 고유진동수에 미치는 영향을 분석하였다.

1. Introduction

Since soil-structure interactions are one of

† Corresponding Author: Member, Dept. of Civil Engineering, Wonkwang University
E-mail : bkleest@wku.ac.kr
Tel : +82-63-850-6718, Fax : +82-63-857-7204
* Dept. of Civil Engineering, Hainan University, Haikou, Hainan, China
** Graduate School, Wonkwang University

the most important structural subjects in the structural engineering, much study concerning the soil-structure interactions had been carried out. Structures related to the soil-structure interactions should be modeled as structures resting on the elastic foundation. One of typical structures related to the soil-structure interactions is the strip foundation which is basically defined as the beam/strip rested on the elastic soil.

During the past few decades, dynamic studies on the strip foundations have been frequently investigated by many researchers. References and their citations include the governing equations and the significant historical literature on the free vibrations of beams resting on elastic soils, i.e. the strip foundations. Briefly, such works included following studies: works dealt with the Winkler soil were discussed by Volterra[1], Panayotounakos and Theocaris[2], Wang and Brannen[3], Eisenberger et. al.[4], Issa[5], Kukla[6], DeRosa[7] and Lee et. al.[8]; works dealt with the Pasternak soil were researched by Wang and Stephens[9], Eisenberger and Clastornik[10], Issa et. al.[11], Yokohama[12], Franciosi and Masi[13] and Lee[14]; and works related to the present study, especially concerning the rotatory inertia and shear deformation, were studied by Wang and Stephens[9], Issa et. al.[11], Yokoyama[12] and Lee et. al.[15].

However, the most objective structures in such studies were the uniform members even though the real structural systems consist of many non-uniform members. Actually, non-uniform members as well as uniform ones are often erected in civil engineering works. Such typical structures include the circular strip foundation which supports various loadings like the buildings, storages and mechanical machines.

At the present time, lack of studies on dynamic problems related to circular strip foundation on Pasternak soil is still found in the literature. On the other hand, accurate predictions of the natural frequencies accompanied with the mode shapes are very important in the design of structures, especially when dynamic loads are subjected. Therefore, there is a need to supplement the literature with practical engineering data for designing the foundation structures.

From these viewpoints, this paper aims to theoretically investigate dynamics of the circular strip foundation and also to present practically engineering data for the design of strip foundation. This paper deals with the free vibration analysis of strips which have the solid rectangular cross-section with variable breadth and constant thickness, i.e. tapered circular strip foundation. In this study, the elastic soil which supports the strip is modeled as Pasternak soil and the variable breadth of the strips is assumed to be varied in the linear functional fashion. Differential equations governing the flexural, out-of-plane free vibrations of such circular strip foundation are derived, in which effects of the rotatory and shear deformation are included although the warping of the cross-section is excluded. Also, boundary conditions of both the hinged and clamped ends are derived. Non-dimensional stress resultants are formulated for presenting the mode shapes in parallel with those of the deformations.

Governing differential equations are numerically solved for obtaining the natural frequencies and mode shapes. In the numerical examples, three end constraints of hinged-hinged, hinged-clamped and clamped-clamped are considered. Effects of the rotatory inertia and elasticity ratio on the natural frequencies are reported. Four lowest natural frequencies according to the variations of system parameters such as subtended angle, breadth ratio, thickness ratio, contact ratio and both foundation and shear parameters, respectively, are reported. Also, typical mode shapes of both deformations and

stress resultants are presented.

2. Circular Strip with Variable Breadth

In general, the cross-sectional shapes of strip foundation should be arbitrary. The solid rectangular cross-section is one of the most frequently used in the foundation engineering, which is chosen in this study. Figure 1 shows the horizontally circular curved strip with the solid rectangular cross-section and its dimensions. The radius and subtended angle are depicted as ρ and α, respectively. The typical point along the center line of strip is defined by the polar coordinates (ρ, θ) in which θ is measured from the radius of left end.

As shown in this figure, the thickness H of the rectangular cross-section is constant along the coordinate θ, while the breadth B varies with θ. Breadths of both far ends($\theta = 0$ and $\theta = \alpha$) are B_a and the breadth at the mid-arc ($\theta = \alpha/2$) is B_c.

For defining the variable breadth B, the breadth ratio m and the thickness ratio n are introduced as follows.

$$m = B_c / B_a \tag{1}$$

$$n = H / B_a \tag{2}$$

It is natural that the variation of breadth should be arbitrary. In this study, the breadth

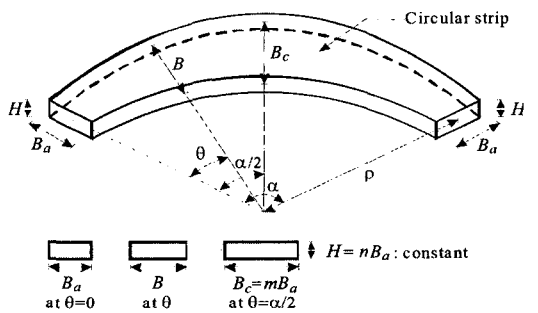

Fig. 1 Circular strip having rectangular cross-section with variable breadth

B is varied in a linear functional fashion with the coordinate θ and is symmetrical about the mid-arc. The equation of B which is a function of θ can now be expressed as follows.

$$B = B_a(c_1 + c_2\theta), \quad 0 \le \theta \le \alpha \tag{3}$$

in which the coefficients c_1 and c_2 for $0 \le \theta \le \alpha/2$ are

$$c_1 = 1, \quad c_2 = (2/\alpha)(m-1) \tag{4a, b}$$

and also the coefficients c_1 and c_2 for $\alpha/2 \le \theta \le \alpha$ are

$$c_1 = 2m-1, \quad c_2 = (2/\alpha)(1-m) \tag{4c, d}$$

Using Eqs. (1)~(4) gives the cross-sectional properties of the area A, second moment of inertia I and torsional constant J of the rectangular cross-section, which will be used for deriving the ordinary differential equations later. The results are

$$A = BH = A_a(c_1 + c_2\theta) \tag{5}$$

$$I = BH^3/12 = I_a(c_1 + c_2\theta) \tag{6}$$

$$J = C_t BH^3 = 4I_a(c_1 + c_2\theta - 0.63n) \tag{7}$$

where $A_a = nB_a^2$ and $I_a = n^3 B_a^4/12$ are the area and second moment of inertia of the cross-section at the two far ends($\theta = 0$ and $\theta = \alpha$), respectively. In Eq. (7), the numerical factor C_t is given as $C_t = (1/3)(1 - 0.63H/B)$, $H/B \le 1$ for the rectangular cross-section[16].

Note that when another functional fashion rather than a linear functional one, e.g. a quadratic function, is chosen, Eq. (3) is merely changed to the selected function and the remaining procedure is the same.

3. Mathematical Model

3.1 Stress Resultants and Inertia Loadings

Shown in Fig. 2 is the circular strip foundation, i.e. circular strip on an elastic soil with the shear layer, namely Pasternak soil, whose cross-sectional properties are already defined in previous chapter. Each end is either hinged or clamped. The dashed line is the un-deformed shape in the static state, while the solid line is one of typical deformed shapes caused by free vibration, which is called as mode shape. Deformation variables of the vertical deflection, rotation due to pure bending, shear distortion and twist angle are denoted by v, ψ, β and ϕ, respectively. Depicted by R_v and R_T due to the Pasternak soil are the vertical and torsional reactions subjected to contact surface between strip and soil, which are discussed in next section 3.2.

Stress resultants which consist of the shear force Q, bending moment M and torsional moment T occur in the cross-section due to deformations of v, ψ, β and ϕ. The shear force related to the shear distortion $\beta = v'/\rho - \psi$ [17] is

$$Q = fGA\beta = fGA(\rho^{-1}v' - \psi) \tag{8}$$

where $(') = d/d\theta$, f is the shape factor of the cross-section and G is the shear modulus of elasticity of the strip material. In case of the rectangular cross-section, the value of f is 0.833.

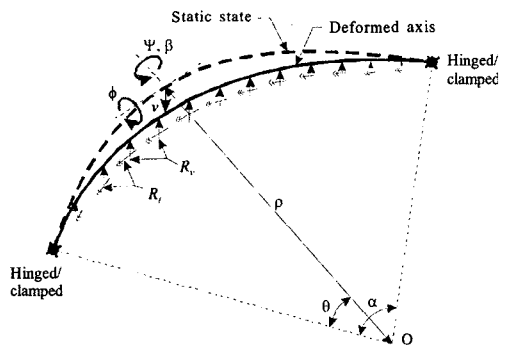

Fig. 2 Circular strip foundation and its variables

The bending and torsional moments are

$$M = \rho^{-1}EI(\phi - \psi') \tag{9}$$

$$T = \rho^{-1}GJ(\psi + \phi') \tag{10}$$

where E is the modulus of elasticity of the strip material.

When the strip is in a state of free vibration, the strip element having mass is subjected to inertia loadings. The free vibration is assumed to be harmonic motion so each coordinate is proportional to $\sin(\omega t)$, where ω is the angular frequency and t is time. The two inertia loadings are flexural inertia force F_v and rotatory inertia C_ψ which are

$$F_v = -\gamma A\omega^2 v \tag{11}$$

$$C_\psi = -\gamma I\omega^2 \psi \tag{12}$$

where γ is the mass density of the strip material.

3.2 Reactions of Foundation

In this paper, the soil foundation is assumed to follow the hypothesis proposed by Winkler and Pasternak. Figure 3 shows the restoring reactions of R_v and R_T due to v and ϕ, respectively, at any coordinate θ. In this figure, B, already defined in Fig. 1, is the breadth of the cross-section. The vertical reaction R_v is caused by the vertical deflection v. The discrepancy of v between out-and in-side extremes of the strip element is obviously caused by ϕ under the assumption that there is no bend along the radial direction. As the result of this discrepancy, the elastic soil has the torsional reaction R_T. It is evident that the pressure of contact surface between strip and soil is varied with r in a linear fashion. Here, r is the coordinate in the radial direction with the origin at the centroid of the

cross-section depicted as o' in Fig. 3.

The relation between the pressure and deflection of the foundation surface at r can be expressed in the form

$$p(r,\theta) = Kz(r,\theta) - (S/a^2)z''(r,\theta), \quad -B/2 \le r \le +B/2 \tag{13}$$

where $p(r,\theta)$ and $z(r,\theta)$ are the pressure and deflection of the contact surface, and K is the modulus of subgrade reaction and S is the shear modulus. Note that former term with K was proposed by Winkler and later one with S by Pasternak.

From Fig. 3, one can find that

$$z(r,\theta) = v - \phi r, \quad -B/2 \le r \le +B/2 \tag{14}$$

Hence, both reactions R_v and R_T at coordinate θ can now be calculated by using Eqs. (13) and (14) as follows.

$$R_v = B\{Kv - (S/\rho^2)v''\} \tag{15}$$

$$R_T = (B^3/12)\{K\phi - (S/\rho^2)\phi''\} \tag{16}$$

3.3 Dynamic Equilibrium Equations

A small element of the strip foundation shown in Fig. 4 defines the positive directions for the three stress resultants, the three inertia loadings and the two soil reactions, in which each dynamic quantity is treated as an equivalent static one. The three equations for "dynamic equilibrium" of the element are

$$\rho^{-1}Q' - F_v - R_v = 0 \tag{17}$$

$$\rho^{-1}M' - Q + \rho^{-1}T + C_\psi = 0 \tag{18}$$

$$\rho^{-1}M - \rho^{-1}T' + R_T = 0 \tag{19}$$

3.4 Governing Differential Equations

To facilitate the numerical studies and to obtain the most general results for this class of problem, the following non-dimensional system parameters are defined.

$$\eta = v/\rho \tag{20}$$

$$b = B_a/\rho \tag{21}$$

$$k = KB_a\rho^4/(EI_a) \tag{22}$$

$$s = SB_a\rho^2/(EI_a) \tag{23}$$

$$g = G/E \tag{24}$$

where η is the normalized deflection, b is the contact ratio between strip and soil at two far ends, k is the foundation parameter, s is the shear parameter and g is the elasticity ratio. And the frequency parameter is defined as

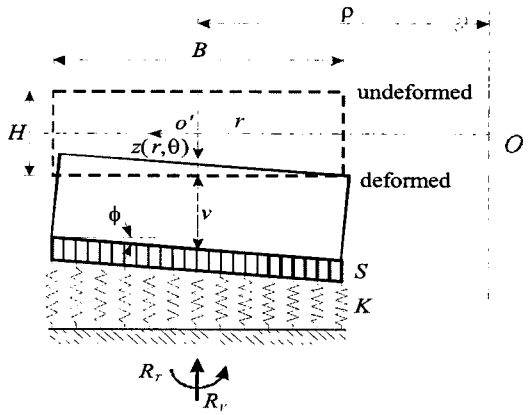

Fig. 3 Reactions of foundation

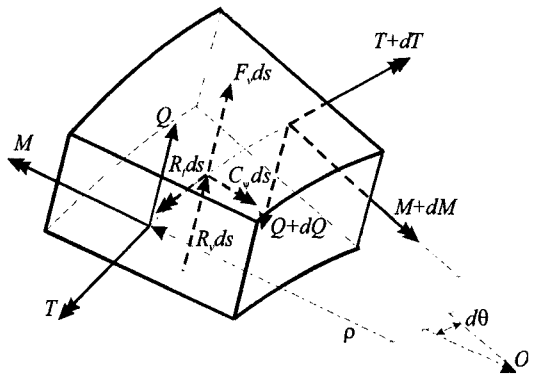

Fig. 4 Loads on strip element

$$C_i = \omega_i \rho^2 \sqrt{\gamma A_a / (EI_a)} \tag{25}$$

which is expressed in terms of the ith frequency $\omega = \omega_i$, $i = 1,2,3,4,\cdots$ where i is the mode number.

The differential equations governing free, out-of-plane vibrations of the strip foundation are derived by using all the equations mentioned above. First, the cross-sectional properties are substituted into the stress resultants, inertia loadings and soil reactions, respectively. Second, the first derivatives of Q', M' and T' are obtained. Third, the stress resultants with the corresponding derivatives, inertia loadings and soil reactions are then substituted into the three equations of dynamic equilibrium. Finally, non-dimensional system parameters are used. The results are

$$\eta'' = e_4\{a_1\eta' + e_1(k - C_i^2)\eta + \psi' - a_1\psi\} \tag{26}$$

$$\psi'' = e_1^{-1}\eta' + a_1\psi' + (e_3a_2 - e_1^{-1} + e_2C_i^2)\psi + (e_3a_2 + 1)\phi' - a_1\phi \tag{27}$$

$$\phi'' = a_4\{-(1 + e_3a_2)\psi' + e_3a_1(\psi + \phi') + (1 + ka_3)\phi\} \tag{28}$$

where the coefficients in Eqs. (26)~(28) are as follows.

$$a_1 = -c_2(c_1 + c_2\theta)^{-1} \tag{29a}$$

$$a_2 = 1 - 0.63n(c_1 + c_2\theta)^{-1} \tag{29b}$$

$$a_3 = (b^2/12)(c_1 + c_2\theta)^2 \tag{29c}$$

$$a_4 = (e_3a_2 + sa_3)^{-1} \tag{29d}$$

$$e_1 = n^2b^2/(12fg) \tag{29e}$$

$$e_2 = -n^2b^2/12 \tag{29f}$$

$$e_3 = 4g \tag{29g}$$

$$e_4 = (1 + e_1s)^{-1} \tag{29h}$$

Note that the differential equations with both $k = 0$ and $s = 0$ are applicable for the flexural, out-of-plane free vibration of circular strip without the soil.

Each end of the strip foundation is either hinged or clamped. The boundary conditions for the hinged end ($\theta = 0$ or $\theta = \alpha$) are given by

$$\eta = 0 \tag{30}$$

$$\psi' = 0 \tag{31}$$

$$\phi = 0 \tag{32}$$

in which Eq. (31) implies the bending moment M is zero at the hinged end.

The boundary conditions for the clamped end ($\theta = 0$ or $\theta = \alpha$) are given by

$$\eta = 0 \tag{33}$$

$$\psi = 0 \tag{34}$$

$$\phi = 0 \tag{35}$$

implying that vertical deflection v and both rotations ψ and ϕ are zero.

For presenting the mode shapes of stress resultants Q, M and T as well as those of deformation v, ψ and ϕ, the non-dimensional stress resultants are formulated as follows.

$$Q^* = Q/(fGA_a) = (c_1 + c_2\theta)(\eta' - \psi) \tag{36}$$

$$M^* = M\rho/(EI_a) = (c_1 + c_2\theta)(\phi - \psi') \tag{37}$$

$$T^* = T\rho/(4GI_a) = \{(c_1 + c_2\theta) - 0.63n\} \times (\psi + \phi') \tag{38}$$

4. Numerical Examples

Since differential equations with the boundary conditions are derived, frequency parameter C_i and both mode shapes of deformations η_i, ψ_i and ϕ_i, and stress resultants Q^*_i, M^*_i and

T^*_i can now be calculated for a given set of system parameters which consists of end constraint, subtended angle α, breadth ratio m, thickness ratio n, contact ratio b, foundation parameter k, shear parameter s, elasticity ratio g and shape factor f (=0.833).

The numerical methods described by Lee et. al.[15] are used to solve the differential equations. First, the Runge-Kutta method is used to integrate the differential Eqs. (26)~(28) subjected to the boundary conditions of Eqs. (30)~(32) or Eqs. (33)~(35). From results of the Runge-Kutta solutions, deformations of η_i, ψ_i and ϕ_i accompanying with those first derivatives can be obtained. Second, the determinant search method combined with the Regula-Falsi method is used to determine the eigenvalues C_i of the differential equations. Finally, mode shapes of the stress resultants Q^*_i, M^*_i and T^*_i are calculated by Eqs. (36)~(38).

For executing the algorithm developed herein, a FORTRAN computer program was written. As the results of numerical analysis, the system parameters such as α, m, n, b, k, s and g are examined in the parametric studies for calculating C_i and mode shapes. Numerical results given in Tables 1, 2 and Figs. 5~10 are now discussed.

Table 1 shows the effect of rotatory inertia on $C_i\,(i=1,2,3,4)$ for the system parameters of α=10, m=1.5, n=0.3, b=0.2, k=5000, s=0.1 and g=0.4. Hereafter, all parameter values including end constraint used in parametric studies are given in tables and figures. When the rotatory inertia is excluded, the coefficient e_2 in Eq. (27) which is related to the rotatory inertia is merely deleted. In Table 1, if rotatory inertia is excluded, $E_R=0$ and otherwise, $E_R=1$. The rotatory inertia always depresses C_i value. Hereafter, the rotatory inertia is included in the numerical examples.

Table 2 shows the effect of elasticity ratio g on C_i. For the construction materials, the g value approximately varies from 0.3 to 0.5. The C_i value increases as the g value is increased. Even though the theoretically largest value of $g(=G/E)$ is 0.5, if the value of g is assumed to be infinite, the effect of shear deformation is neglected in the theory because the shear distortion β expressed in Eq. (8) must become zero and consequently, the total rotation of the cross-section $v'/\rho=\psi+\beta$ should consist of only rotation ψ due to bending. Therefore, the C_i value is overestimated if the shear deformation is excluded in the mathematical model for predicting the natural frequencies. In

Table 1 Effect of rotatory inertia on C_i

End constraint	E_R	Frequency parameter, C_i			
		i=1	i=2	i=3	i=4
Hinged - hinged	0	71.39	80.25	110.0	162.4
	1	71.31	79.81	108.8	160.0
Hinged - clamped	0	72.18	84.77	119.6	175.5
	1	72.08	84.28	118.2	172.5
Clamped - clamped	0	73.55	90.41	130.0	188.9
	1	73.44	89.88	128.5	185.7

* α=1.0, m=1.5, n=0.3, b=0.2, k=5000, s=0.1 and g=0.4

Table 2 Effect of elasticity ratio g on C_i

g	Frequency parameter, C_i			
	i=1	i=2	i=3	i=4
0.30	72.07	84.08	117.0	169.1
0.35	72.08	84.20	117.7	171.0
0.40	72.08	84.28	118.2	172.5
0.45	72.09	84.35	118.6	173.6
0.50	72.09	84.40	119.0	174.5

* Hinged-clamped, α=1.0, m=1.5, n=3, b=0.2, k=5000 and s=0.1

conclusion, it is very important to include the effect of shear deformation in the mathematical model for free vibration problems as this study does.

Figures 5 to 10 show the frequency curves which present the relationships between frequency parameters $C_i (i = 1,2,3,4)$ and system parameters such as α, m, n, b, k and s. In these figures, the value of elasticity ratio $g(= G/E)$ is considered as $g = 0.4$ which approximately corresponds to the typical concrete materials which are frequently used in strip foundation materials. The selected values of system parameters used in the numerical examples presented in these figures are practically acceptable in the foundation engineering.

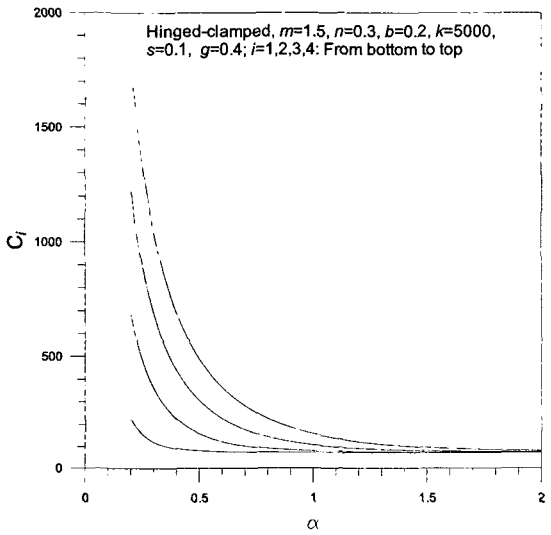

Fig. 5 C_i versus α curves

Figure 5 shows the C_i versus α curves in which C_i value decreases as α is increased. It is fact that the decreasing rate of each frequency curve is greater when the value of α is smaller.

Figure 6 shows relationships between C_i and m. The C_i value decreases as the value of m is increased. However, it is fact that the effect of m on C_i is very minor so that its effect is negligible.

Figure 7 shows the C_i versus n curves. The C_i value increases and reaches peak point and then decreases as the value n is increased. The effect n is more pronounced in the higher mode.

Figure 8 shows the C_i versus b curves in which the C_i value increases and reaches peak point and then decreases as the value b is increased. The effect b is more pronounced in the higher mode.

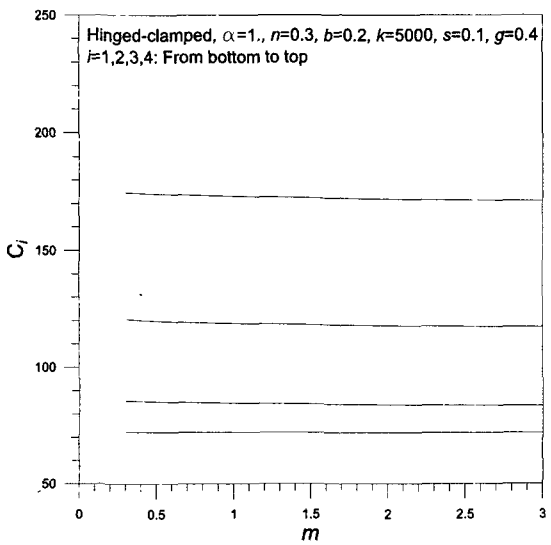

Fig. 6 C_i versus m curves

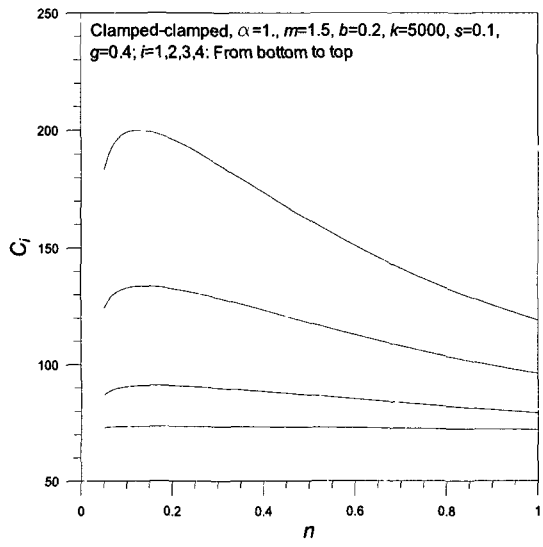

Fig. 7 C_i versus n curves

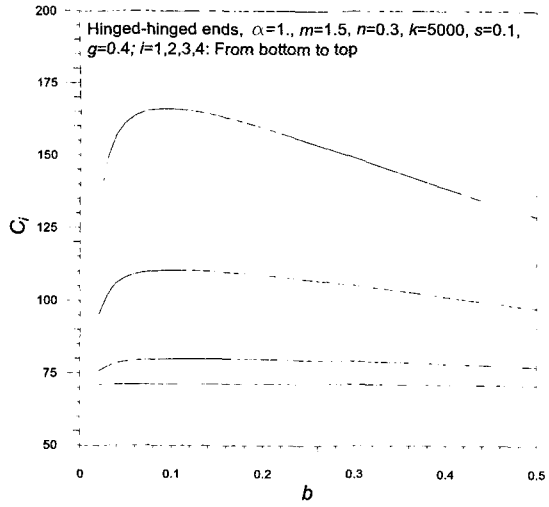

Fig. 8 C_i versus b curves

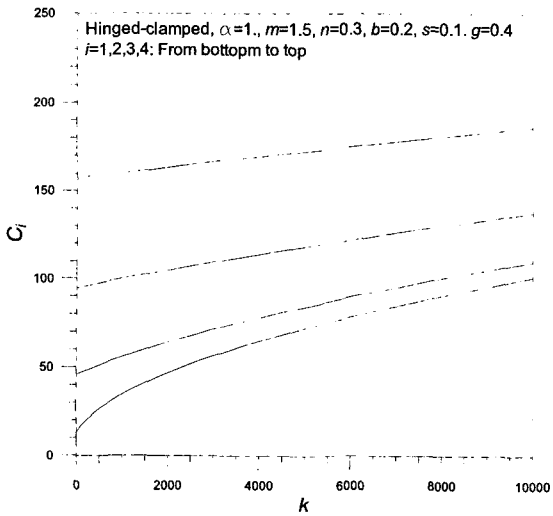

Fig. 9 C_i versus k curves

Figure 9 shows the relationships between C_i and k. The C_i value increase as the value of k is increased.

Table 3 shows the effect of s on C_i in which C_i value increases as the value s is increased. However, it is fact that the effect of s on C_i is very minor so that its effect is negligible.

Figure 10 shows the mode shapes of (a) deformations of η, ψ and ϕ, and (b) stress resultants of Q^*, M^* and T^*. From the mode shapes presented in this figure, positions of the maximum amplitudes and interior nodal points for both deformations and stress resultants can be fully understood. Hence, these kinds of mode shapes can be used in designing strip foundation especially when the dynamic loads are subjected.

Table 3 Effect of shear parameter s on C_i

s	Frequency parameter, C_i			
	i=1	i=2	i=3	i=4
0.0	73.43	89.85	128.5	185.7
0.2	73.45	89.90	128.6	185.8
0.4	73.47	89.95	128.6	185.9
0.6	73.48	90.00	128.7	185.9
0.8	73.50	90.05	128.8	186.0
1.0	73.52	90.10	128.9	186.1

* Clamped-clamped, α=1.0, m=1.5, n=3, b=0.2 and k =5000

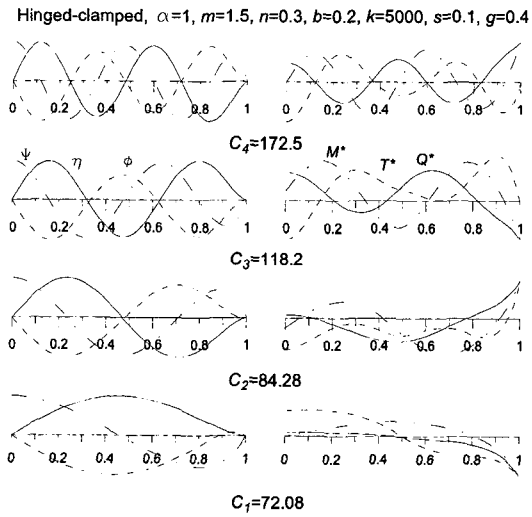

(a) Deformations (b) Stress resultants

Fig. 10 Mode shapes of hinged-clamped ends

5. Experiment

Laboratory-scale circular strip foundation having rectangular cross-section with variable breadth was designed and tested for a

clamped-hinged ends. Materials of the curved strip and foundation are aluminum and rubber, respectively. The geometries, dimensions and material properties of the specimen are: α=70 degree, ρ=0.3 m, B_a=0.03 m, B_c=0.039 m, H =0.006 m, γ=2680 kg/m^3, G=2.6×10^{10} N/m^2, E =6.89×10^{10} N/m^2, E=4×10^6 N/m^3 and S=4.6×10^3 N/m. Thestrip parameters of the specimen are: α=1.22 rad, m=1.3, n=0.2, b=0.1, g=0.38, k =22.6, s=0.33 and f=0.833, with which the frequency parameters C_i were calculated. With these values of C_i, the corresponding frequencies ω_i were calculated from Eq. (25). The predicted natural frequencies for the experimental strip foundation are $F_i = \omega_i/(2\pi)$ =99.86 C_i=15.89 C_i Hz.

Figure 11 shows: (a) a side view of the experimental set-up and (b) the modal analysis system used to measure C_i for the strip foundation in out-of-plane free vibration. The end of a model strip was either clamped between the steel blocks or fastened to a steel hinge, both of which were anchored with bolts to a 5 cm thick Acryl slab glued rubber pad of medium stiffness.

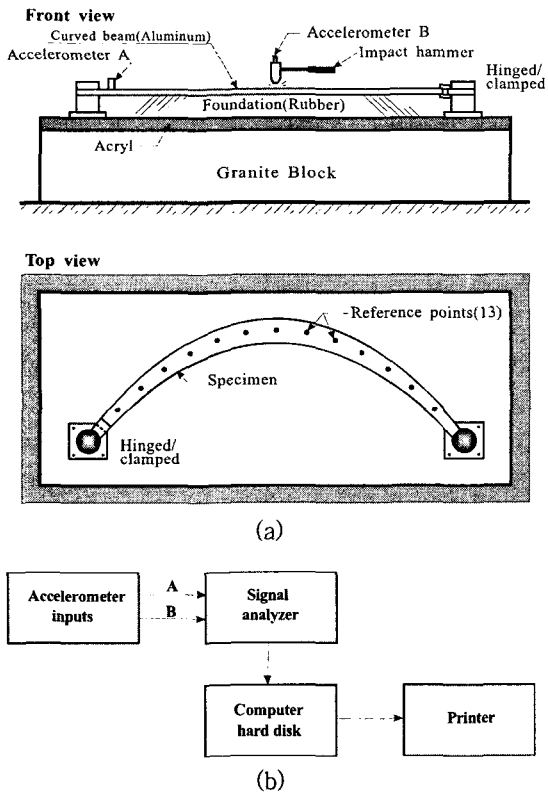

Fig. 11 (a) Experimental set-up and (b) modal analysis system

This experimental design provided low heave and rotational frequencies for the granite block, and offered vibration isolation at the ends. This design minimized the effect of vibration on the end supports so that the experimental frequencies of the strip itself could be identified easily.

In the experiments, 13 reference points were evenly spaced along the top of each strip. As shown in Fig. 11(a), a miniature piezoelectric accelerometer, A, was affixed to the underside of the strip at the reference point nearest to one end.

In a typical experiment, each reference point was struck vertically at the top of the strip with an impact hammer which was fitted with a miniature accelerometer, B. The record of the time history of the out-of-plane response for both accelerometers A and B was obtained. All data were received by a signal analyzer(Model SD390, Scientific-Atlanta Corp.) and processed through a minicomputer using a fast Fourier transform(FFT) analyzer as shown in Fig. 11(b). For data collected for a hammer blow at the location of accelerometer A, the software was used to calculate the frequency spectrum. The peaks of this spectrum occur at the free vibration frequencies of the strip foundation. The reader should be referred to the work of Ewins[18] for more details on the methods of data processing.

The lowest six numerical and experimental results of C_i and F_i are summarized in Table 4.

The frequency spectrum for clamped-hinged ends is presented in Fig. 12. The software gave

Table 4 Comparisons of between theory and experiment (hinged-clamped ends)

i	Theory		Experiment	Deviation (%)
	C_i	F_i (Hz)	F_i (Hz)	
1	9.888	157	141	10.19
2	30.59	485	455	6.19
3	64.68	1026	(923)1112	8.38
4	110.9	1760	1617	8.13
5	169.3	2689	2368	11.93
6	239.1	3799	3275	13.79

* Deviation(%)=(Theory-Experiment)/Theory×100

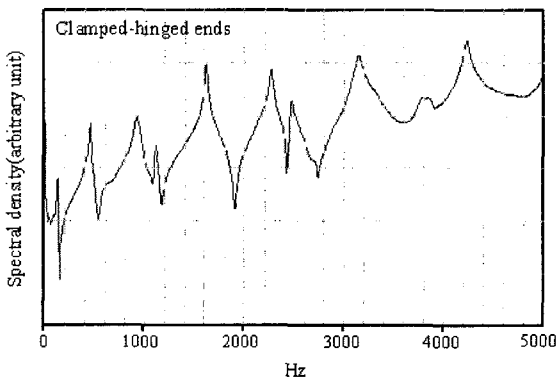

Fig. 12 Free vibration acceleration spectrum for clamped-hinged ends

a listing of the six lowest frequencies corresponding to the first six peaks of each spectrum.

These results, which were reproduced to within about 2 % in repeated tests, are the experimental frequencies listed in Table 4, which shows excellent agreement between the two results obtained from the theory and experiments.

The percentage deviations between theories and experiments in the results average about 9.76 %. From this experimental result, the theories and numerical method were validated.

6. Concluding Remarks

Differential equations governing the flexural free vibrations of circular strip foundation with the variable breadth are derived, in which the elastic soil is modeled as Pasternak soil. The effects of the rotatory and shear deformation are included. Differential equations are solved numerically for calculating the frequency parameters and mode shapes. In the numerical examples, four lowest frequency parameters are calculated. The rotatory inertia always depresses the frequency parameter. The frequency parameter increases as the value of elasticity ratio is increased. Effects of system parameters such as subtended angle, breadth ratio, thickness ratio, contact ratio, and both foundation and shear parameters on the frequency parameters are investigated. The typical mode shapes of stress resultants as well as deformations are presented. Both theories and numerical methods developed herein are robust in the practical ranges of various system parameters. It is expected that the results of this study can be used in designing circular strip foundations especially when the dynamic loads are subjected.

Acknowledgment

The first author appreciates the financial support provided by the Wonkwang University, Korea in 2007.

References

(1) Volterra, E. 1953. "Deflection of Circular Beams Resting on an Elastic Foundation Obtained by the Method Harmonic Analysis", ASME Journal of Applied Mechanics, Vol. 20, pp. 227~237.

(2) Panayotounakos, D. E., Theocaris, P. S., 1980, "The Dynamically Loaded Circular Beam on an Elastic Foundation", ASME Journal of Applied Mechanics, Vol. 47, pp. 139~144.

(3) Wang, T. M., Brannen, W. F., 1982, "Natural Frequencies for Out-of-plane Vibrations of Curved Beams on an Elastic Foundation", Journal of Sound

and Vibration, Vol. 84, pp. 241~246.

(4) Eisenberger, M., Yankelevsky, D. Z., Adin, A., 1985, "Vibrations of Beams Fully or Partially Supported on Elastic Foundations", Earthquake Engineering and Structural Dynamics, Vol. 13, pp. 651~660.

(5) Issa, M. S., 1988, "Natural Frequencies of Continuous Curved Beams on Winkler-type Foundation", Journal of Sound and Vibration, Vol. 127, pp. 291~301.

(6) Kukla, S., 1991, "Free Vibration of a Beam Support on a Stepped Elastic Foundation", Journal of Sound and Vibration, Vol. 149, pp. 259~265.

(7) De Rosa, M. A., 1995, "Free Vibrations of Stepped Beams with Intermediate Elastic Foundation", ASME Journal of Applied Mechanics, Vol. 19, pp. 1~4.

(8) Lee, B. K., Huh, Y., Lee, J. K., 2004, "Free Vibrations of Circular Strip Foundations with Variable Breadth", Transactions of the Korean Society of Noise and Vibration Engineering, Vol. 14, No. 3, pp. 230~235.

(9) Wang, T. M., Stephens, J. E., 1977, "Natural Frequencies of Timoshenko Beams on Pasternak Foundation", Journal of Sound and Vibration, Vol. 51, pp. 149~155.

(10) Eisenberger, M. C., 1987, "Beam on Variable Two-parameter Elastic Foundation", Journal of Engineering Mechanics, Vol. 113, pp. 1454~1466.

(11) Issa, M. S., Nasr, M. E., Naiem, M. A., 1990, "Free Vibrations of Curved Timoshenko Beams on Pasternak Foundations", International Journal of Solids and Structures, Vol. 26, pp. 1243~1252.

(12) Yokohama, T., 1991, "Vibration of Timoshenko Beam-columns on Two-parameter Elastic Soils", Earthquake Engineering and Structural Dynamics, Vol. 20, pp. 355~370.

(13) Franciosi, C., Masi, A., 1993, "Free Vibrations of Foundation Beams on Two-parameter Elastic Soil", Computer & Structures, Vol. 47, pp. 419~426.

(14) Lee, B. K., 1994, "Free Vibration Analysis Beams on Elastic Foundations with Shear Layer", Journal of Korean Society of Steel Structures, Vol. 6, No. 3, pp. 107~115.

(15) Lee, B. K., Oh, S. J., Park, K. K., 2002, "Free Vibrations of Shear Deformable Circular Curved Beams Resting on Elastic Foundations", International Journal of Structural Stability and Dynamics, Vol. 2, No. 1, pp. 77~97.

(16) Timoshenko, S. P., Goodier, J. N., 1951, Theory of Elastic Stability, McGraw-Hill Book Company, USA.

(17) Timoshenko, S. P., 1921, "On the Correction for Shear of the Differential Equation for Transverse Vibrations of Prismatic Bars", Philosophical Magazine, Vol. 41, pp. 744~746.

(18) Ewin, D. J., 1985. Modal Testing: Theory and Practice, John Wiley & Sons, Inc.